Ceramics-Silikáty 63 (4), 399-402 (2019)
www.ceramics-silikaty.cz doi: 10.13168/cs.2019.0036

EFFECT OF MnO_2 ON THE ELECTRICAL PROPERTIES OF 0.96KNNT–0.04BNZ LEAD-FREE PIEZOELECTRIC CERAMICS

WENQIN LUO, #ZONGYANG SHEN

Energy Storage and Conversion Ceramic Materials Engineering Laboratory of Jiangxi Province, China National Light Industry Key Laboratory of Functional Ceramic Materials, School of Materials Science and Engineering, Jingdezhen Ceramic Institute, Jingdezhen 333403, China

#E-mail: shenzongyang@163.com

Submitted June 6, 2019; accepted August 6, 2019

Keywords: Lead-free ceramics, Piezoelectric properties, KNN, MnO_2 dopinge

$0.96(K_{0.49}Na_{0.51})(Nb_{0.97}Ta_{0.03})O3–0.04Bi_{0.5}Na_{0.5}ZrO_3$ + x mol. % MnO_2 (0.96KNNT–0.04BNZ + x mol. % MnO_2, x = 0, 0.1, 0.2, 0.4, 0.6, 0.8) lead-free piezoelectric ceramics were prepared via conventional solid state method. The effect of MnO_2 doping content on the structure and electrical properties of 0.96KNNT-0.04BNZ ceramics was investigated. All samples had pure perovskite structure with coexistence of orthorhombic and tetragonal phases at room temperature. The 0.96KNNT–0.04BNZ + 0.2 mol. % MnO_2 ceramic sample exhibited enhanced piezoelectric constant (d_{33} = 330 pC/N) and planar electromechanical coupling coefficient (k_p = 38.8 %). In addition to other optimized electrical properties such as medium high dielectric permittivity ($(\varepsilon_{33}^T)/\varepsilon_0$ = 1370) and mechanical quality factor (Q_m = 135), relatively low dielectric loss (tan δ = 2.4 %) and high Curie temperature (T_c = 305 °C), this ceramic sample should be a promising lead-free alternative to toxic lead-based piezoelectric materials.

INTRODUCTION

Lead contained piezoelectric materials, typically represented by $Pb(Zi,Ti)O_3$ (PZT) and $Pb(Mg,Nb)O_3$-$PbTiO_3$ (PMN-PT), have been widely applied in sensors, actuators, and transducers due to their excellent electrical properties [1-3]. However, the toxic element Pb is harmful to the environment and human health, and the legislation will be enacted to reduce the Pb content in electronics and other consumer products in the near future. Therefore, developing lead-free piezoelectric ceramics has attracted much interest because of rising environmental and social concerns [4-6].

$(K,Na)NbO_3$ (KNN)-based ceramics are considered as one of the most promising lead-free alternatives to replace lead-based ceramics and have been extensively studied in the past decade [7-17]. One crucial studying direction in KNN-based ceramics is to establish the orthorhombic-tetragonal (O-T) phase boundary near room temperature by A- and/or B-site modification to enhance piezoelectric properties. For example, A-site Li^+, B-site Ta^{5+} and Sb^{5+} modified KNN with O-T phase boundary around room temperature is reported to having enhanced piezoelectric constant d_{33} of ~300 pC/N [7-12]. Moreover, a new rhombohedral-tetragonal (R-T) phase boundary has been developed in $(Bi,Na,K)ZrO_3$ modified KNN-based ceramics, whose piezoelectric properties are reported to be comparable to those of some commercialized PZT ceramics [13, 14]. Actually, we also designed a lead-free $(1–x)(K_{0.49}Na_{0.51})(Nb_{0.97}Ta_{0.03})O_3–xBi_{0.5}Na_{0.5}ZrO_3$ system in our previous work, and an enhanced d_{33} of 317 pC/N was obtained at the composition x = 0.04 accompanied by a high Curie temperature (T_c = 310 °C) [18]. However, other properties of this ceramic sample such as low mechanical quality factor and relatively high dielectric loss need to be further optimized from the viewpoint of commercialized usage.

On the other hand, manganese has been widely reported to improve electrical properties of piezoelectric ceramics, regardless of the introduction form of $MnCO_3$ or MnO_2, whether or not manganese enters the lattice in a stoichiometric ratio or remains at grain boundary in an impurity form [19, 20]. Therefore, in the current research, we choose $0.96(K_{0.49}Na_{0.51})(Nb_{0.97}Ta_{0.03})O_3–$ $–0.04Bi_{0.5}Na_{0.5}ZrO_3$ (0.96KNNT-0.04BNZ) as the base material, while manganese dioxide (MnO_2) is introduced with the target to optimize the piezoelectric properties.

EXPERIMENTAL

Raw materials of analytical reagent grade K_2CO_3, Na_2CO_3, Nb_2O_5, Ta_2O_5, Bi_2O_3, ZrO_2 and MnO_2 from Sinopharm Chemical Reagent Co. Ltd., Shanghai, China were combined in our system $0.96(K_{0.49}Na_{0.51})(Nb_{0.97}Ta_{0.03})O_3$-$0.04Bi_{0.5}Na_{0.5}ZrO_3$ + x mol. % MnO_2 (0.96KNNT-0.04BNZ + x mol. % MnO_2, x = 0, 0.1, 0.2,

0.4, 0.6, 0.8) to prepare ceramic sample by conventional processing route. The raw materials were weighed for each composition and mixed for 24 h in zirconia ball mill at a speed of 120 rpm using absolute ethanol medium. The mixture was calcined at 850 °C for 4 h and then ground again for 24 h. After drying, the polyvinyl alcohol solution (PVA, 5 wt. %) as a binder was added to the calcined powders for granulation. Disks (13 mm in diameter by 1.2 mm thick) were formed by pre-pressing at 100 MPa, and then followed by a cold isostatic pressing. After preheating for 2 h at 650 °C to remove PVA binders, the pellets were sintered for 3 h between 1090 °C and 1130 °C in an ambient atmosphere with a heating rate of 5 °C·min^{-1}, and then furnace cooling to room temperature.

X-ray diffraction (XRD, D8-Advance, CuK$_\alpha$ radiation) was applied to analyze the phase structure of polished sintered ceramic samples. Scanning electron microscope (SEM, JSM-6700F) was used to observe the microstructural characteristics of polished and thermally etched surface of sintered ceramics. For electrical measurements, both sides of the specimens were polished and painted with silver pastes, and then fired for 20 min at 800 °C to form electrodes. Weak-field dielectric constant and loss at 1 kHz as a function of temperature from room temperature to 500 °C were measured by a precision impedance analyzer (HP4294A, Agilent), joining a controlled-temperature cell. For piezoelectric measurements, the samples were poled at 130 °C for 30 min in silicone oil bath applied with an electric field of 30 ~ 40 kV·cm^{-1}. A quasi-static d_{33} meter (ZJ-3A) was used to measure piezoelectric constant d_{33}. The planar electromechanical coupling coefficient was determined by resonance method based on IEEE standard on piezoelectricity [21]. Room temperature polarization-electric field (P-E) loops were observed on a radiant precision workstation (TRek model 609B) using standard Sawyer and Tower circuits.

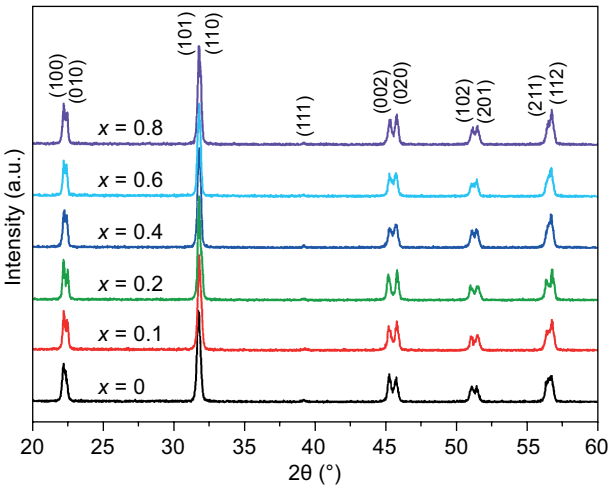

Figure 1. XRD patterns of 0.96KNNT–0.04BNZ + x mol. % MnO_2 ceramics.

RESULTS AND DISCUSSION

As seen from the XRD patterns of 0.96KNNT–0.04BNZ + x mol. % MnO_2 ceramics shown in Figure 1, all ceramic samples are indexed pure perovskite structure, and no impurities can be observed within the detection limit of XRD technique. The splitting diffraction peaks (002) and (020) near 45° are approximately equal in height, indicating that all samples are polymorphic phase transition (PPT) structure with coexistence of orthogonal-tetragonal phases [9, 10]. Meanwhile, no obvious diffraction peak shifting is observed with the increase of MnO_2 doping content, which should be related to low doping content of MnO_2 (< 0.8 mol. %) and similar ionic radius between Mn^{4+} (r_i = 0.053 nm, CN = 6) and Nb^{5+} (r_i = 0.064 nm, CN = = 6) [22].

Figure 2 shows the piezoelectric constant d_{33}, planar electromechanical coupling coefficient k_p and mechanical quality factor Q_m of 0.96KNNT-0.04BNZ + + x mol. % MnO_2 ceramics. With the increase of x value, the d_{33} and k_p first slightly increase and then drop down, presenting peak values of 330 pC/N and 38.8 %, respectively for the composition with x = 0.2. However, the Q_m is found to increase monotonously with the increase of MnO_2 doping content. This phenomenon may be due to the hard doping effect of MnO_2. The replacement of Nb^{5+} by Mn^{4+} in B-site will produce oxygen vacancies, and the oxygen vacancy will make the domain wall movement more difficult, thus increasing the Q_m of the ceramic sample [23].

The dielectric permittivity and loss tan δ of 0.96 KNNT–0.04BNZ + x mol. % MnO_2 ceramics are shown in Figure 3. It can be seen that the variation tendency of with MnO_2 doping content is the same as that of d_{33} and k_p, showing a peak value of 1370 when x = 0.2. The enhanced dielectric permittivity should make some contribution to the increase of piezoelectric constant according to the basic theory of ferroelectrics [24]. The dielectric loss tan δ shows a reverse trend to dielectric constant, having a lowest value of 2.4 % for the ceramic sample with x = 0.2.

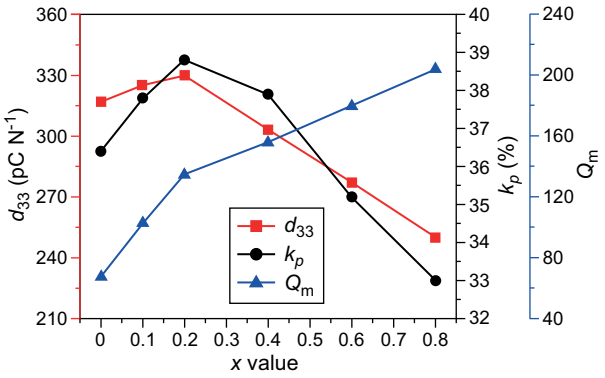

Figure 2. The d_{33}, k_p and Q_m of 0.96KNNT–0.04BNZ + x mol. % MnO_2 ceramics as a function of x values.

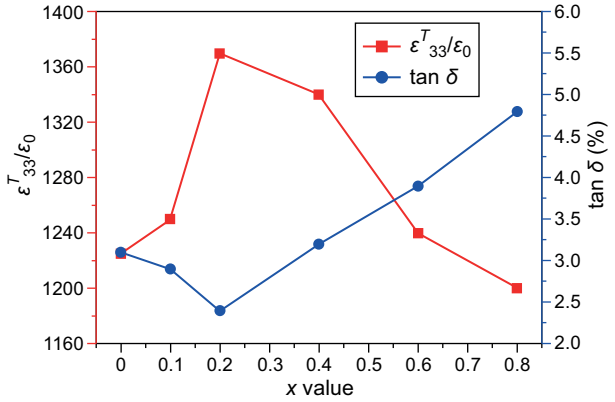

Figure 3. The ($\varepsilon^T_{33}/\varepsilon_0$ and tan δ of 0.96KNNT–0.04BNZ + x mol.% MnO_2 ceramics as a function of x values.

Figure 4 gives the P-E hysteresis loops of 0.96 KNNT–0.04BNZ + x tan mol. tan % MnO_2 ceramics. All ceramics have well saturated hysteresis loop under an applied electric field of 40 kV·cm^{-1}. Basically, the remnant polarization P_r slightly decreases, while the coercive field E_c increases with the increase of MnO_2 doping content, which may also be related to the hard doping effect induced by Mn addition.

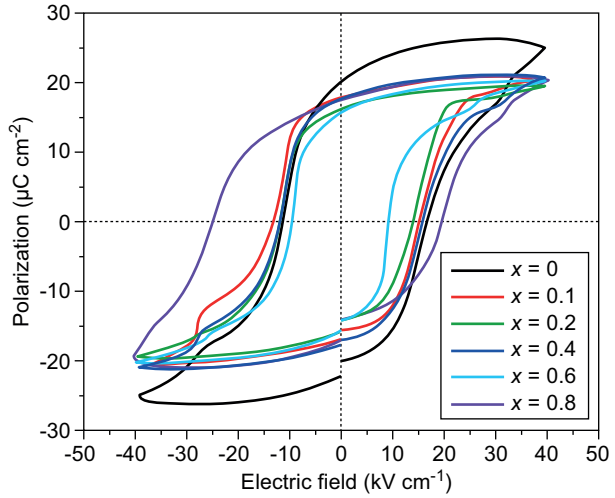

Figure 4. *P-E* hysteresis loops of 0.96KNNT–0.04BNZ + + x mol.% MnO_2 ceramics.

The temperature dependent dielectric constant of 0.96KNNT-0.04BNZ + x mol. % MnO_2 ceramics is shown in Figure 5. It can be seen that all ceramic samples undergo two different phase transitions corresponding to the orthorhombic-tetragonal (T_{o-t}) and tetragonal-cubic (T_c) respectively [25, 26]. With the increase of MnO_2 doping content, the T_c can be detected shifting very slightly towards lower temperature, indicating that Mn^{4+} should incorporate into B-site of perovskite lattice. However, according to the inset of Figure 5, the T_{o-t} around room temperature is almost the same in spite of different MnO_2 addition. For the 0.96KNNT–0.04BNZ + 0.2 mol. % MnO_2 ceramic sample with optimized piezoelectric properties, a relatively high T_c of 305 °C is obtained promising for practical applications as lead-free candidate ceramic materials.

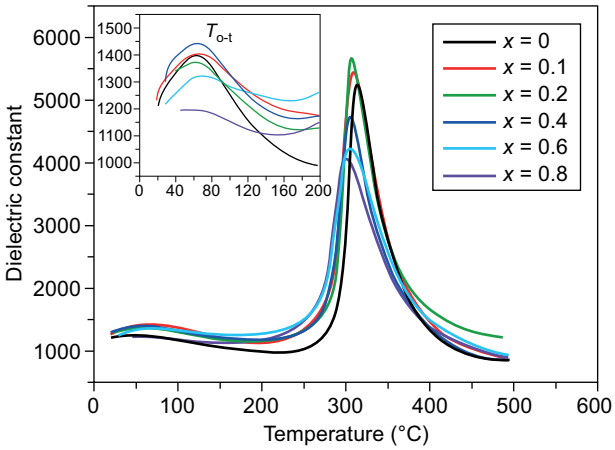

Figure 5. Temperature dependent dielectric constant of 0.96 KNNT–0.04BNZ + x mol. % MnO_2 ceramics. The inset shows an expanded view from room temperature to ~180 °C.

CONCLUSIONS

In this work, the effect of MnO_2 addition on the structure and electrical properties of 0.96KNNT–0.04BNZ ceramics was investigated. Mn^{4+} should be incorporated into B-site of perovskite lattice, and can enhance dielectric and piezoelectric properties of the ceramics within a certain doping level. The 0.96KNNT–0.04BNZ + 0.2 mol. % MnO_2 ceramic sample shows optimized properties as follows: d_{33} = 330 pC/N, k_p = 38.8 %, Q_m = 135, = 1370, tan δ = 2.4 %, P_r = 19.5 μC cm^{-2}, E_c = = 13.9 kV·cm^{-1} and T_c = 305 °C, providing a good lead-free candidate ceramics for piezoelectric applications.

Acknowledgments

This work was financially supported by National Natural Science Foundation of China (61671224) and Science Foundation of Jiangxi Provincial Education Department of China (GJJ160919).

REFERENCES

1. Jaffe B., Cook W. R., Jaffe H. (1971). Piezoelectric Ceramics, Academic, New York.
2. Shung K. K., Cannata J. M., Zhou Q. F. (2007): Piezoelectric materials for high frequency medical imaging applications: A review. Journal of Electroceramics, 19, 139-145. Doi: 10.1007/s10832-007-9044-3

3. Zhang S., Li F., Jiang X., Kim J., Luo J., Geng X. (2015): Advantages and Challenges of Relaxor-$PbTiO_3$ Ferroelectric Crystals for Electroacoustic Transducers – A Review. Progress in Materials Science, 68, 1-66. Doi: 10.1016/j.pmatsci.2014.10.002
4. Saito Y., Takao H., Tani T., Nonoyama T., Takatori K., Homma T., Nagaya T., Nakamura M. (2004): Lead-free piezoceramics. Nature, 432, 84-87. Doi: 10.1038/nature 03028
5. Rödel J., Li J. F. (2018): Lead-free piezoceramics: Status and perspectives. MRS Bulletin, 43, 576-580. Doi: 10.1557/ mrs.2018.181
6. Bell A. J., Deubzer O. (2018): Lead-free piezoelectrics-The environmental and regulatory issues. MRS Bulletin, 43, 581-587. Doi: 10.1557/mrs.2018.154
7. Dai Y., Zhang X., Zhou G. (2007): Phase transitional behavior in $K_{0.5}Na_{0.5}NbO_3$–$LiTaO_3$ ceramics. Applied Physics Letters, 90, 262903. Doi: 10.1063/1.2751607
8. Akdogan E. K., Kerman K., Abazari M., Safari A. (2008): Origin of high piezoelectric activity in ferroelectric $(K_{0.44}Na_{0.52}Li_{0.04})Nb_{0.84}Ta_{0.1}Sb_{0.06}O_3$ ceramics. Applied Physics Letters, 92, 112908. Doi: 10.1063/1.2897033
9. Shen Z. Y., Zhen Y., Wang K., Li J. F. (2009): Influence of Sintering Temperature on Grain Growth and Phase Structure of Compositionally Optimized High-Performance Li/Ta-Modified $(Na,K)NbO_3$ Ceramics. Journal of the American Ceramics Society, 92, 1748-1752. Doi: 10.1111/j.1551-2916.2009.03128.x
10. Zuo R., Fu J., Lv D. (2009): Phase Transformation and Tunable Piezoelectric Properties of Lead-Free $(Na_{0.52}K_{0.48-x}Li_x)(Nb_{1-x-y}Sb_yTa_x)O_3$ System. Journal of the American Ceramics Society, 92, 283-285. Doi: 10.1111/j.1551-2916.2008. 02871.x
11. Wang K., Li J. F. (2010): Domain engineering of lead-free Li-modified $(K,Na)NbO_3$ polycrystals with highly enhanced piezoelectricity. Advanced Functional Materials, 20, 1924-1929. Doi: 10.1002/adfm.201000284
12. Gao Y., Zhang J., Qing Y., Tan Y., Zhang Z., Hao X. (2011): Remarkably Strong Piezoelectricity of Lead-Free $(K_{0.45}Na_{0.55})_{0.98}Li_{0.02}(Nb_{0.77}Ta_{0.18}Sb_{0.05})O_3$ Ceramic. Journal of the American Ceramics Society, 94, 2968-2973. Doi: 10.1111/j.1551-2916.2011.04468.x
13. Wang X., Wu J., Xiao D., Zhu J., Cheng X., Zheng T., Zhang B., Lou X., Wang X. (2014): Giant piezoelectircity in potassium-sodium niobate lead-free ceramics. Journal of the American Chemistry Society, 136, 2905-2910. Doi: 10.1021/ja500076h
14. Zheng T., Wu H., Yuan Y., Lv X., Li Q., Men T., Zhao C., Xiao D., Wu J., Wang K., Li J.F., Gu Y., Zhu J., Pennycook S.J. (2017): The structural origin of enhanced piezoelectric performance and stability in lead free ceramics. Energy & Environmental Science, 10, 528-537. Doi: 10.1039/ C6EE03597C
15. Zhang M., Wang K., Du Y., Dai G., Sun W., Li G., Hu D., Thong H.C., Zhao C., Xi X., Yue Z., Li J.F. (2017): High and Temperature-Insensitive Piezoelectric Strain in Alkali Niobate Lead-free Perovskite. Journal of the American Chemistry Society, 139, 3889-3895. Doi: 10.1021/jacs. 7b00520
16. Li P., Zhai J., Shen B., Zhang S., Li X., Zhu F., Zhang X. (2018): Ultrahigh Piezoelectric Properties in Textured $(K,Na)NbO_3$-Based Lead-Free Ceramics. Advanced Materials, 30, 1705171. Doi: 10.1002/adma.201705171
17. Li P., Huan Y., Yang W., Zhu F., Li X., Zhang X., Shen B., Zhai J. (2019): High-performance potassium-sodium niobate lead-free piezoelectric ceramics based on polymorphic phase boundary and crystallographic texture. Acta Materialia, 165, 486-495. Doi: 10.1016/j.actamat.2018. 12.024
18. Shen W., Shen Z. Y., Li Y., Wang Z., Liu H. (2015): Structure and Electrical Properties of $(1-x)(K_{0.49}Na_{0.51})(Nb_{0.97}Ta_{0.03})O_3$-$xBi_{0.5}Na_{0.5}ZrO_3$ Lead-free Piezoelectric Ceramics. Journal of Synthetic Crystals, 44, 2793-2797.
19. Wang X., Liang P., Chao X., Yang Z. (2015): Dielectric Properties and Impedance Spectroscopy of $MnCO_3$-Modified $(Ba_{0.85}Ca_{0.15})(Zr_{0.1}Ti_{0.9})O_3$ Lead-Free Ceramics. Journal of the American Ceramics Society, 98, 1506-1514. Doi: 10.1111/jace.13481
20. Chen L., Fan H., Zhang S. (2017): Investigation of MnO_2-doped $(Ba,Ca)TiO_3$ lead-free ceramics for high power piezoelectric applications. Journal of the American Ceramics Society, 100, 3568-3576. Doi: 10.1111/jace.14894
21. Meeker T. R. (1996): Publication and proposed revision of ANSI/IEEE standard 176-1987. IEEE Transactions on Ultrasonics Ferroelectrics and Frequency Control, 43(5), 717-772.
22. Shannon R. (1976): Revised effective ionic radii and systematic studies of interatomic distances in halides and chalcogenides. Acta Crystallographica Section A, 32, 751-767. Doi: 10.1107/S0567739476001551
23. Yao F., Zhang M., Wang K., Zhou J., Chen F., Xu B., Li F., Shen Y., Zhang Q., Gu L., Zhang X., Li J. F. (2018): Refreshing Piezoelectrics: Distinctive Role of Manganese in Lead-Free Perovskites. ACS Applied Materials & Interfaces, 10, 37298-37306. Doi: 10.1021/acsami.8b14958
24. Damjanovic D. (1998): Ferroelectric, dielectric and piezoelectric properties of ferroelectric thin films and ceramics. Reports on Progress in Physics, 61, 1267-1324. Doi: 10.1088/0034-4885/61/9/002
25. Shirane G., Newnham R., Pepinsky R. (1954): Dielectric Properties and Phase Transitions of $NaNbO_3$ and $(Na,K)NbO_3$. Physics Review, 96, 581-588. Doi: 10.1103/PhysRev. 96.581
26. Shen Z. Y., Li Y., Jiang L., Li R., Wang Z., Hong Y., Liao R. (2011): Phase transition and electrical properties of $LiNbO_3$-modified $K_{0.49}Na_{0.51}NbO_3$ lead-free piezoceramics. Journal of Materials Science: Materials in Electronics, 22, 1071-1075. Doi: 10.1007/s10854-010-0261-1